



## Modeling An In-Pipe Inspection Robot

Pancho Dachkinov<sup>1</sup>, Ivan Chavdarov<sup>2</sup>, Veselin Pavlov<sup>1</sup>

<sup>1</sup>Technical University – Sofia, Kliment Ohridski № 8 Str., Sofia, Bulgaria

<sup>2</sup>Institute of Systems Engineering and Robotics  
Bulgarian Academy of Sciences,  
Acad. G. Bonchev Str., Bl.1113, Sofia, Bulgaria

**Abstract.** An original construction of a mobile robot for in-pipe inspection with six contact areas to the pipe is introduced. The components of the robot are made by a 3D printer. The robot has four driving vehicles and elastic elements for make contact with the pipe walls. The loads in the contact areas are defined. This is an important condition for the locomotion of the robot in the pipe and at different angles. The results are also presented graphically. Experiments for overcoming complex routes were done.

**Keywords:** Mobile Robot, In-pipe Inspection, Pipes, 3D Printer

### 1. INTRODUCTION

The pipelines are the most commonly used tool for fluid transfer – liquids or gas. Over time, however, a lot of problems appear in such systems. Most of these problems are associated with the conditions of the pipes such as corrosion, mechanical deformations, etc. Therefore, regular control and maintenance is necessary. There are a lot of ways and methods for pipe inspection and in recent years the application of mobile robots has been increased (Roh et al., 2005). One big advantage of the robots is that they can reach pipes with small diameter and also can be equipped with electronic devices such as sensors, lights and cameras for the pipe inspection requirements in hardly accessible and/or dangerous (explosive, aggressive, noxious) routes (Tache et al., 2007). Many of these robots are designed for a specific, specific application, therefore the requirements and features of the pipe inspection robots are also specific.

The requirements of these types of robots come from specific features of the pipes and goals which they have to perform (Na et al., 2010). The maneuverability has a leading position and depends on the configuration of the pipeline. The pipelines usually contain horizontal and/or vertical pipes but there are also

branches, valves, etc. (Ahrary, 2009). Other damages and different obstacles are possible, which are not mentioned in the technical documentation. Because of these reasons, robots for pipe inspection must have a flexible and reliable construction. There is a diversity of pipes with different standardized diameters, a lot of manufacturing technologies for pipes and different shapes, different pipe geometry and sections, etc.

The pipes often have complex space geometry. Furthermore, it is necessary to overcome different tilts and curves with different radiuses. Diameter changes and branches which could have heterogeneous shapes and dimensions, could cause essential problems (Li et al., 2007). There are problems with communications in metal pipes and also energy transfer in long routes. An autonomous, battery power supply is recommended. Sagging, which changes the sections geometry, appears in long pipes.

These conditions create some of the requirements for pipe inspection robots:

- Movement in pipes with different diameters;
- Movement in pipelines with curves ( $\geq 90$  [°]);
- Possibility for movement in branches;

- Exit from various unexpected situations by changing its shape and geometry (re-configuration of the robot's body);
- To be moisture and pollution resistant;
- Changing the rotation of the motors in order to return to the same route. Therefore, symmetric geometry of the robot in the locomotion direction;
- Enough forces and torque for moving in vertical pipes.

Missions of that type of robots are connected with checking the reliability, coverings, welding seams (by ultrasound flaw for in-pipe-inspection robots), corrosion, pollution, etc. In some cases, it is necessary for the robot to eliminate problems. That is why the robot must be maneuverable, equipped with sensor systems, tools, etc. Often, a precise navigation system is required for determining the exact location of the robot.

## 2. THEORETICAL BASIS AND DESCRIPTION OF THE ROBOT

### 2.1. Design of the Robot

The robot will have constant contact with the pipe in six areas. The body of the robot changes its geometry according to the diameter of the pipe, the radius of the curve, overcoming obstacles and optimizing the pressure of the wheels by using elastic elements. The robot consists of four wheel-legs which have a propeller shape and are shown on Fig. 1, position (1).

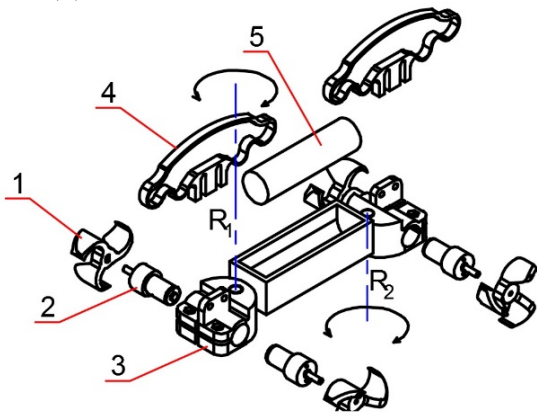


Fig. 1. Structure of the robot

The wheels follow the diameter of the pipe (Fig. 2) and are made of material called Fila

Flex via 3D Printer. They are driven by four DC motors with implemented spur gear (element 2 on Fig.2) with gear ratio 298:1 which decreases the speed for the needs of the in-pipe inspection and increases the torque aiming to overcome curves and vertical sections and roughness. The body (3) of the robot is printed by a 3D Printer from a material called PLA. The body includes two vertical joints  $R_1$  and  $R_2$  which are printed directly assembled.

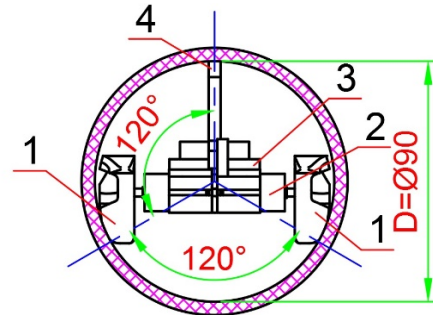


Fig. 2. Placement of the robot in the pipe

This mobility allows adaptation for overcoming obstacles and locomotion in curves with small radius (Fig. 3).

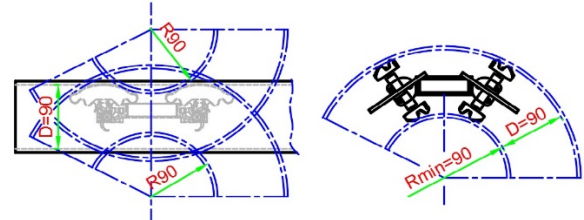


Fig. 3. Curve adaptation

The robot is powered by a charging battery (4,2 [V]) (5). The last major component of the construction is shown on position (4). These are two thin elastic plates created by a 3D Printer from PLA. These plates are used for permanent contact of the wheel (1) with the pipe. In the future, these plates will have controllable height which will improve the pressure and therefore the locomotion of the robot.

### 2.2. Theoretical Basis

In order to design that type of robots it is important to define the forces that affect the robot during its movement (Jun et al., 2004). In order to define the friction forces between the wheels, the elastic elements and the pipe,

it is necessary to know the pressure at those sections. On Fig. 4 the movement of the robot in a tilt section on angle  $\alpha$  and with constant diameter  $D$  is shown. A strongly simplified model is represented, where the elastic elements are replaced by one equivalent force and the robot platform is accepted as a static construction – beam on two supports **A** and **B**.

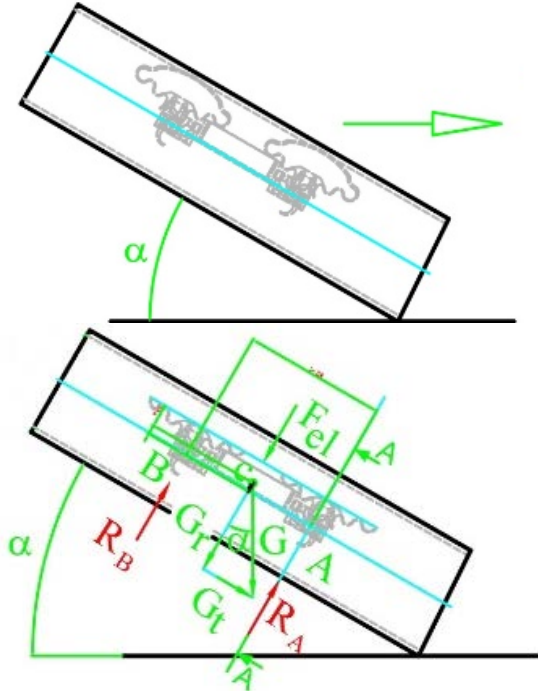


Fig. 4. Forces in tilt overcoming

It is accepted that the contact is at a point. From that model the pressure is defined. For the more loaded one (motor) **A** is received:

$$R_A = \frac{0.5 * L * F_{el}}{L} + \frac{0.5 * L * G_r + (0.5 * D + e) * G_t}{L} \quad (1),$$

$$= 0.5 * F_{el} + \frac{0.5 * L * G_r + (0.5 * D + e) * G_t}{L}$$

$$= R_{Af} + R_{Ag}$$

where:  $G_r = G \cos(\alpha)$  – radial component of the gravity force;  $G_t = G \sin(\alpha)$  – axial component of the gravity force;  $D$  is the inside pipe diameter;  $L$  and  $e$  are dimensions shown on Fig. 4,  $\alpha$  is the tilt angle of the pipe.  $R_{Af}$  and  $R_{Ag}$  – represent the influence of the elastic and the gravity forces on the pressure at point **A**.

The result for the reaction  $R_A$  (formula 1) is an intermediate step for the final loadings

of the wheels. To define the full loading, it is necessary to analyze the robot in cross section of the pipe. If the robot is not rotated to the horizontal axis  $Y$  (shown on Fig 5a)), the forces in the two wheels  $R_{A1}$  and  $R_{A2}$  are equal and could be easily defined

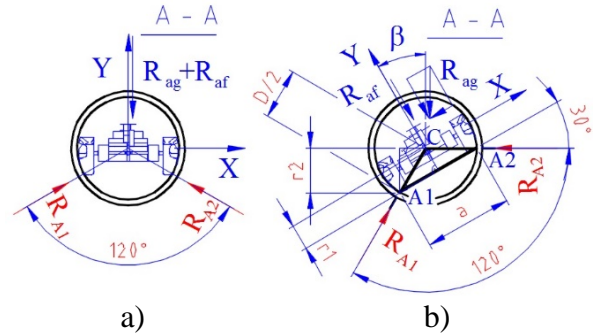


Fig. 5. Alignment of the forces in a cross section of the pipe

Then the elastic and the gravity forces impact evenly on the wheels:

$$R_{A1} = R_{A2} = \frac{R_{Af} + R_{Ag}}{2} \quad (2).$$

The construction of the robot allows theoretically the contact points to be aligned evenly on angle  $120 [^\circ] \left( \frac{5\pi}{6} rad \right)$  to the center **c** of the pipe. A more complex case is when the robot is rotated at an angle  $\beta$ , twisted to the direction of the locomotion (Fig. 5b). Then from the laws of the statics it follows:

$$R_{A1} = \frac{(R_{Af} + R_{Ag}) * \sin(\beta) * 0.5 * \alpha - R_{Ag} * r_2 * \cos(\beta)}{\alpha} \quad (3),$$

$$R_{A2} = \frac{(R_{Af} + R_{Ag}) * \sin(\beta) * 0.5 * \alpha + R_{Ag} * r_2 * \cos(\beta)}{\alpha} \quad (4).$$

Here  $a$  and  $r_2$  are distances shown on Fig. 5b). From the cosine theorem it follows:

$$a = \sqrt{\frac{D^2}{2} - 4 * D * \cos\left(\frac{5 * \pi}{6}\right)} \text{ and } r_2 = \frac{D}{4} \quad (5).$$

The determination of the reactions  $R_{A1}$  and  $R_{A2}$  are the base for defining the resistant forces that the motor needs to overcome.

### 3. DATA

The dimensions of the 3D printed model of the robot are:  $L = 0.122$  [m];  $D = 0.09$  [m];  $e = 0.02$  [m]. The model mass and the elastic force are measured:  $m = 0.187$  [kg]; respectively  $G = m \cdot g = 1.83$  [N];  $F_{el} = 2.07$  [N] – with minimal deformation –  $h_{p0} = 0.01$  [m], matching the most favorable position of the wheels of the robot in a pipe with a diameter  $D = 0.09$  [m] (Fig. 6b)) and  $F_{el} = 3.45$  [N] – with maximal deformation ( $(h_{p0} + h_{p1}) - h_{p2}$ ) –  $0.05$  [m] (Fig. 6a).

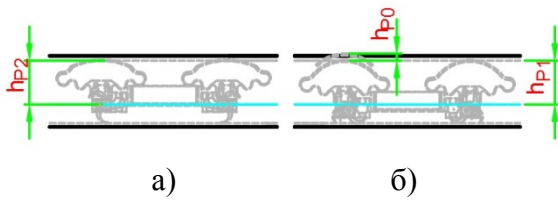


**Fig. 6.** Deformation of the elastic elements

A route is created which has these elements: march from diameter  $D = 0.11$  [m] to  $D = 0.09$  [m] with length of the march  $B = 0.165$  [m]. Curve on  $\pi/4$  [rad] and  $\pi/2$  [rad], with radius  $R = 0.11$  [m], with horizontal, tilt and vertical position. These elements could be combined with each other, which gives a lot of variations for the experiments.

#### 4. EXPERIMENTAL RESULTS

Some experiments were made with a real prototype of the robot and with different pipeline configurations.



**Fig. 7.** An experiment for tilt, curves and match overcoming

The results of the experiment show successfully crossing the march, curves, tilts and even locomotion in vertical sections (Fig. 7).

By using the data from the theoretical force parameters and by variation of the tilt angle  $\alpha$ , the reaction  $R_A$  of the most loaded support (formula 1) could be calculated.

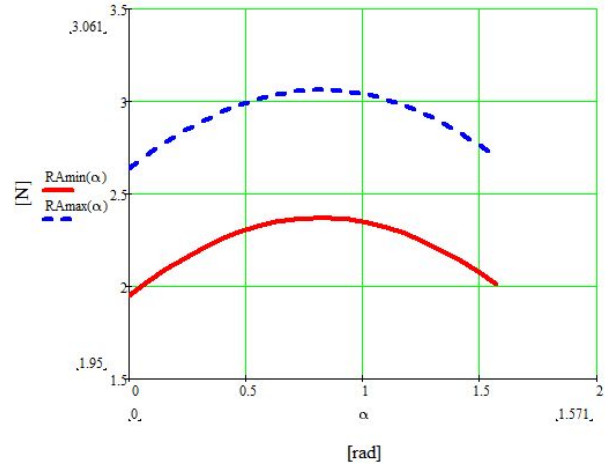


**Fig. 8.** Change of the reaction  $R_A$  by varying the tilt angle  $\alpha$  from  $0$  to  $\frac{\pi}{2}$  [rad].

$R_{Amin}(\infty)$  is defined when the deformation of the elastic element is minimal:  $F_{el} = 2.07$  [N],  $R_{Amax}(\infty)$  is defined when the deformation of the elastic element is maximal:  $F_{el} = 3.45$  [N] (Fig. 8). The maximum value for  $R_A$  is when  $\alpha = 0.8$  [rad].

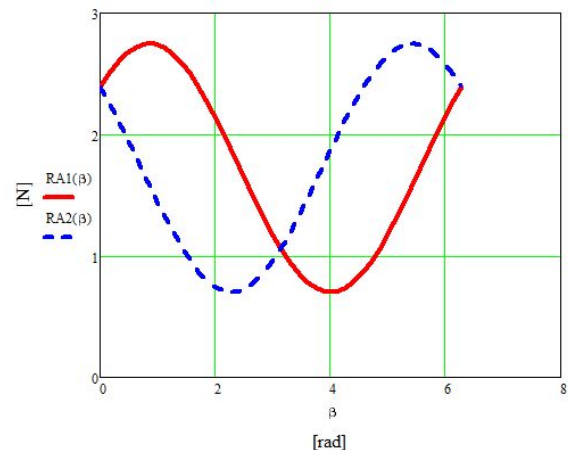


**Fig. 9.** Changes in  $R_{A1}$  and  $R_{A2}$  with variation of the  $\beta$  angle

The change of the normal force in the driving wheels in minimum loading  $F_{el} = 2.07$  [N]

and in a horizontal pipe  $\alpha = 0$  [rad], is shown on Fig. 9. The angle  $\beta$  is varied from 0 [rad] to  $2\pi$  [rad]. The maximum value of  $R_{A1}$  is 2.7 [N] when  $\beta = 1$  [rad] and the minimum value of  $R_{A1}$  is 0.7 [N] when  $\beta = 4$  [rad]. The maximum value of  $R_{A2}$  is 2.7 [N] when  $\beta = 5.5$  [rad] and the minimum value of  $R_{A2}$  is 0.7 [N] when  $\beta = 2.3$  [rad].

## 5. COMMENTS AND CONCLUSIONS

The created robot prototype has good maneuverability and very simple construction. The robot includes only five basic elements (Fig. 1) made by a 3D Printer for a few hours from low cost materials. The body of the robot and the links (passive degrees of freedom) are printed as one component which reduces the assemble operations and the number of the parts. The set of elastic elements increases the flexibility and the cohesion by realizing permanent contact with the pipe, which allows overcoming obstacles and movement in vertical sections. The robot has four independently working motors, which create enough driving force, torque and power. The battery supply of the robot allows easy remote control via computer.

Fig. 9 shows changes in the reactions  $R_{A1}$  and  $R_{A2}$  by variation of the angle of torsion  $\beta$ . It is shown that when  $\beta = 0 \pm 2\pi$  [rad], the orientation of the robot is the same as on Fig. 5a) and support reactions are equal. When  $\beta = \pi \pm 2\pi$  [rad], they are equal again but this time with lower value, because in this case the robot is rotated with the wheels up and the gravity force is subtracted. For all other  $\beta$  angle values the reactions are different. The two graphics on Fig. 9 are the same but phased at an angle  $120$  [°] ( $\frac{3}{4}\pi$  [rad]).

The force statics analysis shows how the forces in the system are positioned. It also allows several orientations of the robot in the pipe to be analyzed. The real deformations and forces in the elastic elements (wheels (1) and plates (4)) could hardly be defined. The mechanical characteristics of the elastic elements – both the wheels and the plates are nonlinear and the orientation of the wheels to the plates is random. The contact zone be-

tween the elastic elements and the pipe is not at a point as it is accepted and it changes with time. Because of these reasons, the results from the statics analysis are approximate.

However, it is considered that these results could be used in the design phase of that type of robots. For this purpose, the states of maximum and minimum loading should be defined. These states could be used to define the optimal cohesion in locomotion in vertical sections of the pipe and whether the motors have enough torque to overcome the highest resistance.

The project is in its initial phase and a couple of problems should be solved. For example, the possibility to choose a route or the effect of the moisture and the pollution. It is necessary to equip the robot with sensors and cameras and also to change the rotation direction of the motors. At last but not least, the robot should have a system for remote control.

## ACKNOWLEDGEMENTS

This paper was published with the support of the Institute of Systems Engineering and Robotics, BULGARIAN ACADEMY OF SCIENCES.

## REFERENCES

- Ahrary, A., 2009, Localization of a mobile robot in sewer pipes using hough transform, *ICGST-GVIP Journal*, ISSN 1687-398X, Volume (9), Issue (I), February 2009, pp 17–23  
<http://ofuturescholar.com/paperpage?docid=658791>
- Bio-mimetic robots, 2010, World Academy of Science, *Engineering and Technology*, 61 2010, pp 18–24.  
<http://waset.org/publications/5960/development-of-a-pipeline-monitoring-system-by-bio-mimetic-robots>  
<http://ieeexplore.ieee.org/document/4399074/?reload=true&arnumber=4399074>
- <https://e-collection.library.ethz.ch/eserv.php?pid=eth:7824&dsID=eth-7824-01.pdf>
- International conference on robotics and biomimetics, 2004, August 22–26, 2004, Shenyang, China, pp 119–124.
- Jun, C., Deng, Z., Jiang, S., 2004, Study of Locomotion Control Characteristics for Six Wheels Driven In-Pipe Robot, *Proceedings of the 2004 IEEE*

- Li, P., Ma, S., Li, B., Wang, Y. & Ye C., 2007, An In-pipe Inspection Robot based on Adaptive Mobile Mechanism: Mechanical Design and Basic Experiments , *Proceedings of the 2007 IEEE/RSJ International Conference on Intelligent Robots and Systems* , San Diego, CA, USA, Oct 29 – Nov 2, 2007, pp 2576–2581.
- Na, S., Shin, D., Kim J., Jung J. & Won Y., 2010, *Development of a pipeline monitoring system*, Nov 1, 2010.
- Roh, S. & Choi, H. R., 2005, Differential-Drive In-Pipe Robot for Moving Inside Urban Gas Pipelines, *IEEE TRANSACTIONS ON ROBOTICS*, VOL. 21, NO. 1, FEBRUARY 2005, pp 1–17.  
<http://ieeexplore.ieee.org/abstract/document/1391010/authors>
- Tache, F., Fischer, W., Moser, R., Mondada, F., Siegwart, R., 2007, Adapted Magnetic Wheel Unit for Compact Robots Inspecting Complex Shaped Pipe Structures, ©2007 IEEE, pp 1–6